Generation of long-range, near-cut-on guided resonances in composite panels

Christophe Droz, Olivier Bareille, Mohamed N Ichchou

Generation of long-range, near-cut-on guided resonances in composite panels

Christophe Droz,* Olivier Bareille, and Mohamed N. Ichchou
Vibroacoustics & Complex Media Research Group,
LTDS - CNRS UMR 5513, École Centrale de Lyon, France
(Dated: October 31, 2018)

In this paper near-cut-on Guided Resonances (GR) are generated in a composite structure using an array of piezoelectric transducers. A GR is a type of high-order uni-directional wave mode, guided between the finite boundaries of a periodic waveguide's cross-section. Near their cut-on frequency, these waves often exhibit high chromatic dispersion and spatial decay, which compromise their potential use for wave-based inspection and Structural Health Monitoring (SHM) of advanced composite or metamaterials. A custom GR actuator is designed to achieve an accurate shape appropriation of the predicted 3D Floquet-Bloch solutions in a 3m-long sandwich structure. An original wave conversion phenomenon is then exploited to generate almost non-dispersive selected GR pulses near their cut-on frequency. Full wavefield measurements are conducted in time-domain using Laser Doppler Velocimeter to provide new insights on the GR near-cut-on scattering effects in the low vibroacoustic bandwidth.

I. INTRODUCTION

The propagation of elastic waves in complex structures have been the subject of intense research in the last decades, particularly driven by the development of non-destructive testing (NDT) (e.g. in pipes [1] and rails [2, 3]), or the development of embedded structural health monitoring (SHM) systems for the critical aircraft and aerospace components [4–6]. In this field, wave-based techniques are still promised to a variety of applications [7], such as predictive maintenance solutions for critical infrastructures and automated defect evaluation [8, 9]. The prediction of propagative phenomena has also become more challenging, due to the increasing complexity of new lightweight components employed in aerospace and transportation industry. These structures are often based on advanced composites, which involve either heterogeneous assemblies or periodic patterns. An abundant literature can also be found on bio-inspired [10], meta-materials [11, 12] or locally resonant waveguides [13], to cite a few. In these structures, the prediction of guided waves raises challenging issues as well, such as the appearance of local modes or highly scattering behaviors above the first Brillouin zone. In automotive and aerospace industries, similar phenomena can typically be encountered in the low- or medium frequency ranges [14], since a variety of macro-scale periodic designs [15, 16] can be used to enhance a structure's vibroacoustic properties.

In this context, the development of numerical methodologies able to study wave propagation in continuous or periodic waveguides from a unit-cell analysis, has given new insights on wave's physics inside these structures. One popular implementation is known as the Wave Finite Element Method (WFEM) [17–19]. One can cite among recent examples the wave scattering effects in undulated [20], textile composites [21], honeycomb [22, 23] or poroelastic [24] waveguides. Implementations of the WFEM also extends to uncertain or slowly varying [25, 26], piezoelectric [27] or locally resonant metamaterials [28, 29].

More importantly, the development of model order reduction strategies (e.g. [30–32]) has allowed the handling of large unit-cell FE models. In particular it has given researchers the ability to handle the entire finite cross-section of large-scaled 1D waveguides, such as helicopter rotor blades, acoustic pipes, complex ducts or stiffened panels. Consequently, it is now possible observe a variety of complex wave phenomena, broadening the concepts of Bloch waves and from which Lamb and ring modes can be regarded as a peculiar subclass of waves. One usually defines the concept of guided resonance as the mode of a waveguide's finite cross-section, propagating as a plane wave along its main direction. These waves can be seen as a generalization of high-order circumferential modes, well-known in axi-symmetric structures, to any kind of uni-directional waveguide exhibiting a finite cross-section. Numerical investigations recently shown that these waves could be of interest in the fields of SHM, energy harvesting or for wave beaming applications. In composite sandwiches, the authors recently [33] shown that well chosen low-frequency GR exhibit higher sensitivities to small-scaled damages than classical waves, even generated at higher frequencies.

However, apart from the aforementioned Lamb and ring modes [34–37], and the recent investigations of Serey et al. [38] on ultrasonic wave mode selection, such guided resonances have been seldom, if ever, generated experimentally in composites. To the authors' knownledge, GR have never been studied, nor observed near their cut-on frequencies. Despite the recentness of applications for selective GR techniques, the lack of literature on the topic can be explained by the many practical challenges raised by the generation of guided resonances within the low acoustic bandwidth: 1) The selective generation of a complex guided resonance requires the design of a cus-

* christophe.droz@gmail.com

tom actuation system and a prior computation of its dispersion characteristics and deformed shape. Otherwise additional propagating or evanescent waves may be produced as well. Actuation systems based on ring arrays of embedded ultrasonic transducers have been extensively used for guided wave testing applications in pipes. However the proposed actuation strategy is more similar to mode force appropriation techniques [39, 40] in the understanding that generating a guided resonance can be seen as the appropriation of a cross-sectional wave shape within a bandwidth predicted by its dispersion curves. 2) In the proposed realization, the same waveform must be actuated within a broad bandwidth, below and above the cut-on frequencies. Therefore the actuation system has to produce higher loads than for standard modal appropriation techniques. 3) Lamb waves are usually exploited above their cut-on frequency, hence often exhibit very low dispersion (A0, S0 and all first-order waves are considered as having a cut-on at 0 Hz). The present work challenges the generation of long-range guided resonances close to their cut-on frequency, i.e. near their zero group velocity. Dispersion curves therefore have to be thoroughly analyzed to identify bandwidths where transient pulses can be generated with low dispersion.

This paper describes the design strategy and implementation of an array of piezoelectric actuators on a carbon-reinforced sandwich panel, in order to investigate the generation of guided resonances in the low vibroacoustic bandwidth. A periodic model of the panel is developed in Sec.II A, where the material properties are retrieved using state-of-the-art wave-based methodologies [22, 41]. In Sec.II B the periodic unit-cell model is then processed through a WFE Framework to analyze wave dispersion characteristics and investigate veering and deformed shapes of the guided resonances. A concept of piezoelectric system is then introduced in Sec.III to achieve waveform appropriation and generate a 8^{th}-order bending guided resonance (GR 8). The system is implemented on the composite panel in III B. The propagation, conversion and dispersion of generated guided resonances is eventually measured using full-field velocimetry in Sec.IV and the various scattering effect occurring within the cut-on bandwidth are interpreted. Some conclusions are drawn in Sec.V with guidelines for the efficient generation of guided resonances in arbitrarily complex waveguides.

II. ANALYSIS OF GUIDED RESONANCES IN THE COMPOSITE WAVEGUIDE

A. Description and modeling of the composite panel

The composite structure is a 600×2890 mm sandwich panel made of a 10 mm-thick Nomex honeycomb core (ECA, 3.2 mm cell size) surrounded by two 0.6 mm-thick, 3-plies CFR skins. The panel has free edges and is oriented in the vertical position, where x, y and z axes refer to the panel's length, width and normal directions, respectively. Wave-based methods are preferred to measure equivalent material properties of large-scaled structures in the mid-frequencies. These in-situ characterization techniques provide important mechanical parameters (i.e. tensile modulus of the skins and equivalent transverse shear modulus of the core layer) within the typical dynamic range where guided resonances are observed: between 1 kHz and 5 kHz. Mechanical parameters of the sandwich panel are retrieved using Transition Frequency Characterization (TFC) [22] and Inhomogenenous Wave Correlation (IWC) [41] methods. A finite element model of the waveguide's representative unit-cell is built based on the results presented in table I.

The periodic unit-cell is modeled using FEM with a regular mesh involving 80 linear 3D brick elements along the width and 12 elements in the core's thickness. This mesh (see Figure 3) corresponds to a minimum of 10 elements per wavelength for the highest wavetype's order predicted at 5 kHz and 20 elements per wavelength for the solution analyzed in Section III. The total number of degrees of freedom of the representative periodic 3D unit-cell is 6318.

B. Prediction of guided resonances using unit-cell modeling

The WFEM exploits periodic structure theory to derive the propagation constants Λ and eigenvectors Ψ from the direct Bloch formulation:

$$[\mathbb{D}_{RL}(\omega)\Lambda^{-1} + (\mathbb{D}_{RR}(\omega) + \mathbb{D}_{LL}(\omega)) + \mathbb{D}_{LR}(\omega)\Lambda]\Psi = 0 \quad (1)$$

where the dynamic stiffness sub-matrices are denoted $\mathbb{D}_{ab}(\omega) = \mathbb{K} + j\omega\mathbb{C} - \omega^2\mathbb{M}$ with a and b the left and right sides of the unit-cell while we denote $\mathbb{K}$, $\mathbb{C}$ and $\mathbb{M}$ the finite element stiffness, damping and mass matrices of the periodic cell. Interested reader can refer to [18, 19, 30] for details regarding the WFEM, computational issues and reduced formulations. The propagating solutions are derived from the dispersion analysis (e.g. the complex wavenumbers and group velocities) using the filtering criterion $0.95< |\lambda| <1$ and are shown in Figures 2 and 1. A wavematching procedure is used to distinguish the 18 wave types: 4 first-order (or fundamental) waves (associated with flexural, torsional, longitudinal and shear motions) appearing at 0 Hz, 2 high-order shear/longitudinal and 12 high-order flexural waves for which cut-on frequencies are listed in table II. In the following, we use the notation *'GR n'* to denote the nth-order transverse vertical-polarized *guided resonance*. The subset of high-order in-plane waves is therefore not included in the chosen 'GR' nomenclature and GR 2 stands for the wave with the first cut-on frequency at 206 Hz in table II. The first- and second-order longitudinal and shear waves cutting-on around 3.3 kHz

Component	Density (kg.m^{-3})	Young's modulus (Pa)	Shear modulus (Pa)	Poisson coefficient
Core	ρ=96	$E_x = 2\times10^6$	$G_{xz} = 36.5\times10^6$	$\nu_{yz} = 0.02$
		$E_y = 2\times10^6$	$G_{yz} = 52.9\times10^6$	$\nu_{xz} = 0.02$
		$E_z = 0.54\times10^9$	$G_{xy} = 2\times10^6$	$\nu_{xy} = 0.48$
Skins	ρ=1440	$E_x = 69.8\times10^9$	$G_{yz} = 1\times10^9$	$\nu_{yz} = 0.15$
		$E_y = 69.8\times10^9$	$G_{xz} = 1\times10^9$	$\nu_{xz} = 0.15$
		$E_z = 1\times10^9$	$G_{xy} = 1\times10^9$	$\nu_{xy} = 0.05$

TABLE I. Material properties of the sandwich panel. The honeycomb core is represented as an homogeneous medium and an equivalent loss factor $\eta = 0.2\%$ is assumed in the composite plate. Added mass due to the reflexive tapes (see Sec.III) is included in the upper density.

have higher velocities and are not visible in figure 1.

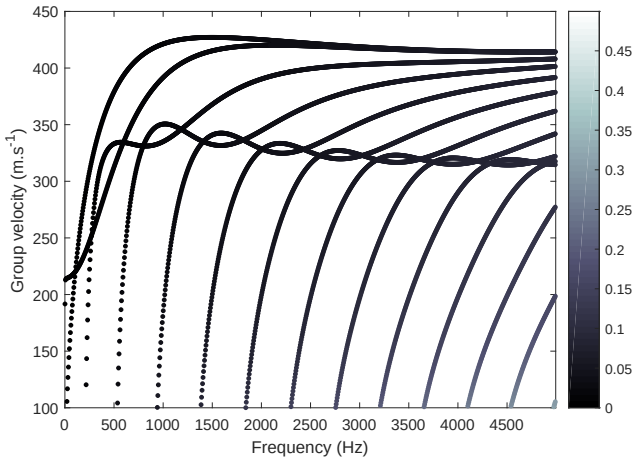

FIG. 1. Group velocities of guided waves in the sandwich structure. Colorbar represents imaginary part of the complex wavenumbers, which indicates wave attenuation.

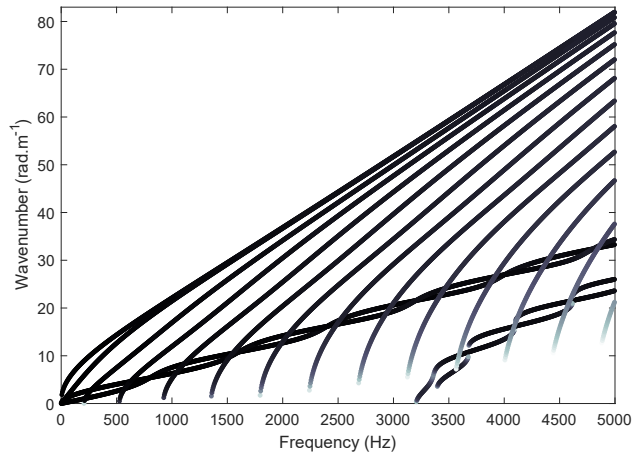

FIG. 2. Wavenumbers of guided waves in the sandwich structure.

Wave	Cut-on (Hz)
Flexural	0
Torsional	0
Longitudinal	0
Shear	0
2nd-order	206
3rd-order	526
4th-order	926
5th-order	1356
6th-order	1796
7th-order	2241
8th-order	**2686**
9th-order	3126
10th-order	3566

TABLE II. Cut-on frequencies of the first flexural propagating waves.

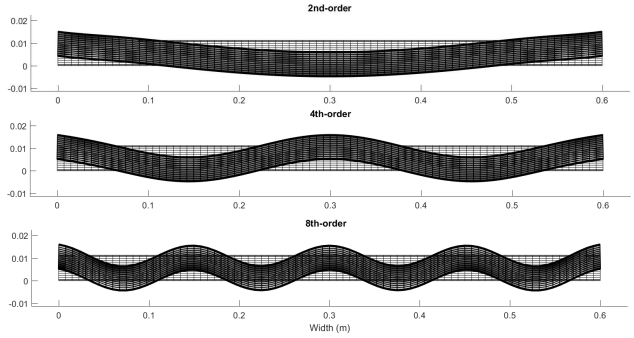

FIG. 3. Deformed shape of GR 2, GR 4 and GR 8 at 4000 Hz.

Although the dispersion curves provide crucial information to choose the input signal's frequency and predict the pulse's dispersion, the knowledge of wave shapes is required to perform selected GR waveform appropriation. The eigenvectors of Eq.(1) represent the nodal distribution of displacements and forces associated with propagating Bloch waves. It is emphasized that the shape of a given wave usually varies with frequency,

due to localization or conversion effects. The deformed shapes of several guided resonances are shown in figure 3 at 4 kHz. At this frequency, the GR 8 wave (whose cut-on occurs at 2686 Hz) has a group velocity $c_{g_8}(4000) = 320\text{m.s}^{-1}$ and a phase velocity $c_{\phi_8}(4000) = 575\text{m.s}^{-1}$. Before reaching their shear asymptotic behavior, guided resonances are subjected to a noticeable veering effect above their cut-on frequencies, as shown in figure 4. This phenomenon yields a smallest frequency-dependence of their group velocities: for GR 8 wave, the predicted group velocity deviates by less than 2% between 3600 Hz and 4800 Hz. Noteworthy, this means that a finite wave pulse generated within this bandwidth is expected to have a lower spatial dispersion than in higher frequencies.

III. DESIGN OF AN EMBEDDED PIEZOELECTRIC TRANSDUCER FOR GR 8 WAVES

In this section, a piezoelectric actuation system is designed to create the GR 8 wave in the composite panel. An array of piezoelectric transducers is the preferred solution for generating high-amplitude elastic waves from an embedded system.

A. Concept of wave-mode appropriation

Modal appropriation techniques (also called phase resonance or normal mode testing) are used to perform stationary modes actuation from a set of distributed external loads. This concept can be applied to perform appropriation on the unit-cell (or cross-section) of a periodic waveguide, enabling the generation of guided resonances at different frequencies, as illustrated in Fig.5. The figure shows how a same GR can be generated at different frequencies, at the condition that the deformed shape of the cross-section (i.e. waveform) remains the same over the considered bandwidth.

Although punctual loads could be distributed at the anti-node locations to create the required waveform, it is preferable to apply bending loads using thin d_{13} piezoelectric patches. Indeed, applied loads have to be distributed more uniformly along the cross-section than for modal appropriation, where a single mode usually exist at a given frequency. The existence of multiple propagating wavetypes with close deformed shapes requires an accurate load distribution. In thick sandwich laminates, high-amplitude bending motions are obtained by applying in-plane loads on opposite skins, as depicted in figure 6. This strategy presents the advantage of facilitating a future embedding of the actuation device while avoiding the excitation of high- or first-order waves.

The design proposed in figure 6 involves 7 patches on each skin and is able to produce 7 anti-node curvatures, corresponding to the GR 8 wave presented in figure 3. The array is installed at a free edge of the structure and each patch is centered on a anti-node location identified by the vertical displacement maximums visible in figure 3, except for the free ends. Although these regions exhibit a slight curvature at 4 kHz, this is not the case close to the cut-on frequency (around 2.7 kHz).

B. Design and embedding on the composite panel

The 14 piezoelectric patches are made of PZT (PIC255) material and are polarized along the vertical direction. The patches are placed on the external upper and lower skins of the sandwich panel at 35.4 mm from the edges and with a 6.2 mm spacing from each other to produce the deformed shape of the GR 8 in figure 3 between 2500 and 4000 Hz. A PVC mold is designed to place and bond the patches at the selected locations using epoxy resin. The design of the mold and the PZT patches' references and dimensions are described in Appendix V. The patches dimensions are 25 mm × 70 mm × 2 mm. The thickness was chosen to provide enough surface stress, avoid break while maintaining minimal added weight of the embedded system. The x-dimension of 25 mm is less than the minimal half-wavelength at 5 kHz in the propagation direction. A picture of the actuator's array is shown in figure 7. The overall weight of the GR actuation system is 0.387 kg (i.e. 9% of the panel's weight).

IV. MEASUREMENT OF TRANSIENT PULSE PROPAGATION

Wavefield measurements can be difficult to achieve on composite plates due to light diffraction produced by the high surface roughness. The plate is therefore tapered using reflexive tapes and measurements are conducted using PSV-400 velocimeter. Given the predicted GR 8 wave cut-on frequency around 2.7 kHz and the group velocity plateau observed between 4 and 4.5 kHz, three pulses will be experimented, with bandwidths centered at 2.5 kHz, 3 kHz and 4 kHz respectively. The input signal is a sine modulated 8-cycles pulse with Hanning window. As amplification may differ between 2.5 and 4 kHz, the signals are normalized using the amplifier's output voltage. Additional information on the test bench is available in [42], including mapped surface velocities, wavefield acquisition methods and post-processing scripts. In the following, time frames are displayed and discussed for each of the three pulse bandwidths.

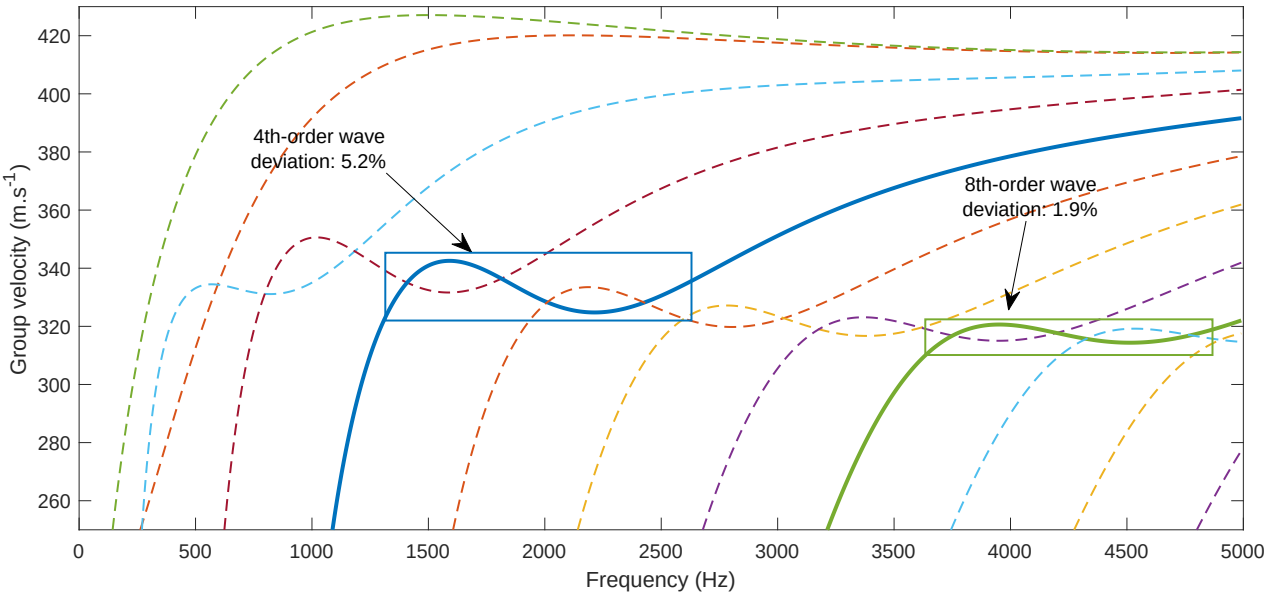

FIG. 4. Conversion effect producing veering of the group velocities for guided resonances. Relative deviations from the mean velocities are computed and highlighted for waves GR 4 (—-) and GR 8 (—-).

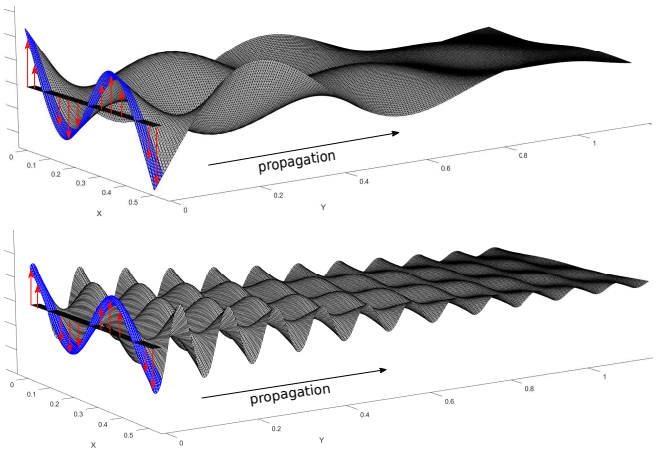

FIG. 5. Principle of wave appropriation: the same wave shape is actuated at two different frequencies (a) and (b), generating different wavelengths in the propagation direction while the transverse horizontal wavelength remains the same. Punctual loads (in red) are applied to create the waveform.

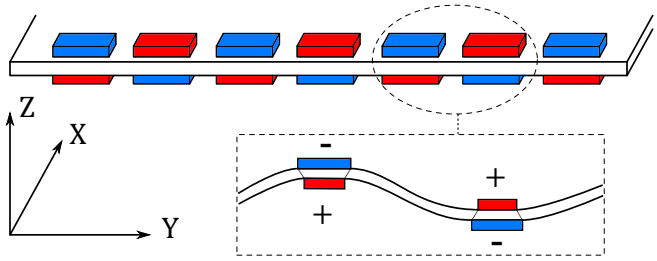

FIG. 6. Principle of bending moment actuation at anti-node locations. Positive (in red) and negative (in blue) signals are used to operate the patches to produce the bending motion. The depicted patch array can produce up to a GR 8 wave.

FIG. 7. Picture of the actuators' array for 8th-order guided resonance actuation.

A. Propagation a guided resonance at 2.5 kHz

Fig. 8 shows the pulse actuation and propagation at 2.5 kHz. Frames 1 and 2 show a good waveform appropriation on the left edge of the plate by the piezoelectric patches, although the actuation occurs below the cut-on frequency. One can note that the symmetry of the wavefield is well maintained in the four time frames. The GR8 pulse is immediately scattered after actuation, while energy propagates under several first-order waves.

A pronounced conversion into even harmonics GR 2 and GR 4 waves can be observed in frames 3-4 while GR 6 is hardly visible. This behavior is consistent with predictions, as the propagation of GR 8 is not expected in this bandwidth and symmetry does not allow the propagation of odd number harmonics. Wavenumbers and phase velocities of GR 2 are in good agreement with the predictions in Fig.2.

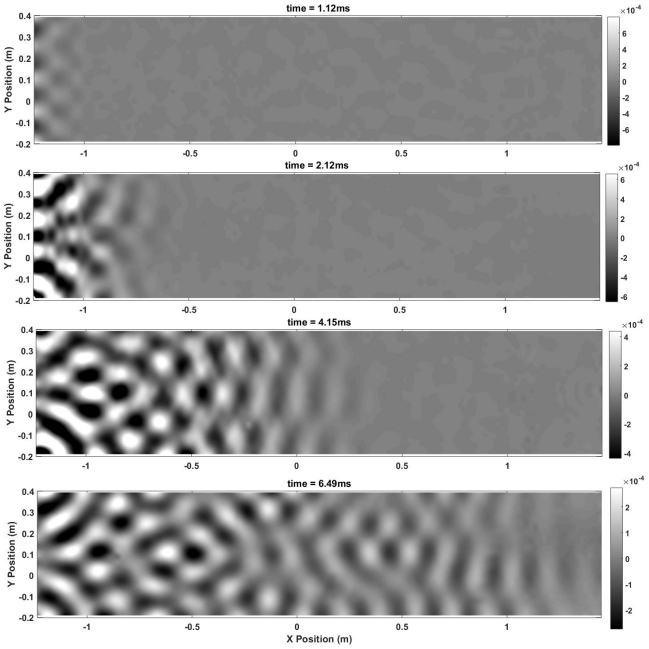

FIG. 8. Transient wave pulse propagation time frames (1.12, 2.12, 4.15, 6.49) ms.

B. Propagation a guided resonance at 3 kHz

Fig. 9 shows the pulse actuation and propagation slightly above the predicted cut-on frequency, at 3 kHz. This time the GR 8 wave propagation is observed along nearly 20 cm before the pulse is scattered. This highly dispersive behavior is consistent with predictions and will be analyzed in more details in Sec.IV C. The the propagation of three sub-harmonics, GR 2, GR 4 and GR 6 is clearly visible from the wavefield as their speeds are different (between 320 - 420 $\mathrm{m.s^{-1}}$ in Fig.4). It should be mentioned that this group velocity pattern differs from Lamb waves, as in the present case the group velocities are always decreasing with a wave's order, except within the plateau bandwidth. This allows straightforward discrimination of the different converted GRs based on their respective time of flight (ToF), where GR 0 (see frame 3 at $x = 0.4$ m in Fig.9) is the fastest wave. Predictions are again confirmed, although the desired GR 8 wave pulse is too dispersive to propagate over the 2.9 m-long structure.

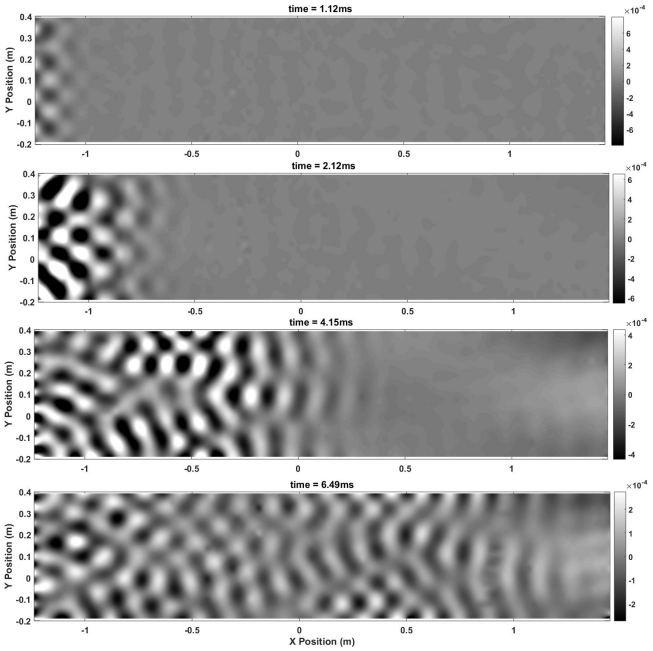

FIG. 9. Transient wave pulse propagation time frames (1.12, 2.12, 4.15, 6.49) ms.

C. Propagation a guided resonance at 4 kHz

The GR 8 wave generated at 4000 Hz is shown in figure 10. Noteworthy, the guided resonance propagates perfectly over nearly 3 meters. A slight frontward conversion into GR 2 and GR 0 occurs while a very little dispersion is observed, thus demonstrating the group velocity plateau predicted around 4 kHz. The phase velocity is easily estimated at 571 $\mathrm{m.s^{-1}}$, which is in good accordance with the predicted dispersion curves ($\mathrm{c}_\phi(4000)$=575 $\mathrm{m.s^{-1}}$). Note that the Group Velocity Dispersion (GVD), $GVD = \dfrac{\partial}{\partial\omega}\left(\dfrac{1}{c_g}\right)$ describing the temporal pulse spreading produced by the chromatic dispersion confirms this results, as the GVD decreases from 7.46 $\mathrm{s^2.m^{-1}}$ at 3 kHz to 0.07 $\mathrm{s^2.m^{-1}}$ at 4 kHz.

V. CONCLUSIONS

In this paper the generation and propagation of near cut-on guided resonances through a composite panel was investigated numerically, then experimentally. Propagation of the GR was examined after its actuation at three frequencies: 2500, 3000 and 4000 Hz. The generation of a GR 8 wave pulse was successfully achieved by cross-sectional wave shape appropriation, using an array of PZT transducers. It is also mentioned that using an array of such PZT actuators can drastically increase the wave amplitude through constructive signal generation. However, the prior knowledge of the GR waveforms and dispersion characteristics is crucial to design such an actuation system. A WFEM algorithm

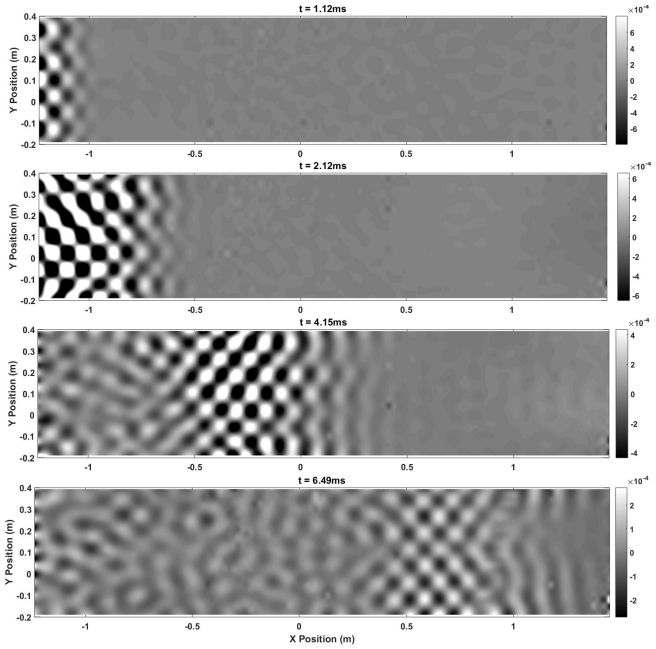

FIG. 10. Transient wave pulse propagation time frames (1.12, 2.12, 4.15, 6.49) ms.

was implemented to compute and analyze wave behavior, while TFC method was used to achieve in-situ structural parameter identification from ToF measurements. The dispersion analysis highlighted the presence of a group velocity plateau bandwidth (around 4 kHz), where near cut-on guided resonances exhibit an almost non-dispersive behavior, despite being close to the wave's cut-on frequency. It is emphasized that the analysis of low-frequency, near cut-on propagation is generally a challenging task, as waves exhibit high group velocity dispersion (GVD), leading a transient pulse to exhibit short-range and highly scattering propagation. This group velocity plateau phenomenon was exploited to achieve the generation and propagation of a GR 8 wave along the nearly 3 m-long sandwich structure, while the pulse was slightly above the cut-on frequency. Measurements were achieved using full-field velocimetry, which provide an interesting insight on the guided resonance transient scattering process in a sandwich composite, as it is emphasized that observed bending-to-shear transition effects only exist in sandwich waveguides. It is hoped that future work will help further understand the near-cut-on scattering process, providing design actuation systems for more complex GR appearing in arbitrarily shaped periodic structures with finite cross-sections.

APPENDIX: MOUNTING STRATEGY FOR THE PIEZOELECTRIC PATCHES

The PZT patches are PI plates with reference C255(wCuNi) of dimensions 70×25×2mm. Patches are bonded using an epoxy resin while a polymer (PVC) mold was designed and manufactured to place and bond the patches. The dimensions of the mold are shown in figure 11, which provide the detailed locations of each patch. The operating limits of the patches is 50 V and the elastic and electro-mechanical parameters can be found in [43].

ACKNOWLEDGMENTS

The authors gratefully acknowledge the support from the European Research Council through the H2020-EJD-VIPER (GA 675441) project. The Labex CeLyA is also acknowledged for their support. The authors would like to thank Stephane Lemahieu and Lionel Charles (Ecole Centrale de Lyon) for their work and contribution during the handling of the experimental set-up and Guillaume Inquiété (Airbus Helicopters) for the fruitful discussions.

REFERENCES

[1] Lowe, M.J., Alleyne, D.N., Cawley, P.. Defect detection in pipes using guided waves. Ultrasonics 1998;36(1):147–154.

[2] Hayashi, T., Song, W.J., Rose, J.L.. Guided wave dispersion curves for a bar with an arbitrary cross-section, a rod and rail example. Ultrasonics 2003;41(3):175–183.

[3] Wilcox, P., Pavlakovic, B., Evans, M., Vine, K., Cawley, P., Lowe, M., et al. Long range inspection of rail using guided waves. In: Review of Progress in Quantitative Non-Destructive Evaluation; vol. 22(1). AIP Publishing; 2003, p. 236–243.

[4] Zhao, X., Gao, H., Zhang, G., Ayhan, B., Yan, F., Kwan, C., et al. Active health monitoring of an aircraft wing with embedded piezoelectric sensor/actuator network: I. defect detection, localization and growth monitoring. Smart Materials and Structures 2007;16(4):1208–1217.

[5] Giurgiutiu, V.. Tuned lamb wave excitation and detection with piezoelectric wafer active sensors for structural health monitoring. Journal of Intelligent Material Systems and Structures 2005;16(4):291–305.

[6] Diamanti, K., Soutis, C.. Structural health monitoring techniques for aircraft composite structures. Progress in Aerospace Sciences 2010;46(8):342–352.

[7] Rose, J.L.. A baseline and vision of ultrasonic guided wave inspection potential. Journal of pressure vessel technology 2002;124(3):273–282.

[8] Song, F., Huang, G., Hudson, K.. Guided wave propagation in honeycomb sandwich structures using a piezoelectric actuator/sensor system. Smart Materials and Structures 2009;18(12):125007.

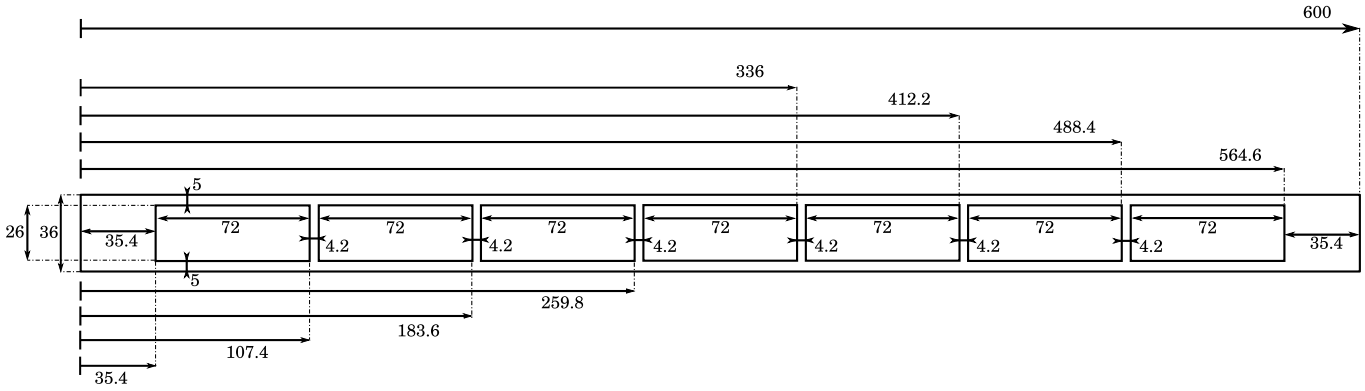

FIG. 11. Dimensions of the mould used to implement the PZT patches for guided resonance actuation.

[9] Raghavan, A., Cesnik, C.E.. Guided-wave signal processing using chirplet matching pursuits and mode correlation for structural health monitoring. Smart Materials and Structures 2007;16(2):355.

[10] Zhang, Q., Yang, X., Li, P., Huang, G., Feng, S., Shen, C., et al. Bioinspired engineering of honeycomb structure–using nature to inspire human innovation. Progress in Materials Science 2015;74:332–400.

[11] Xiao, Y., Wen, J., Yu, D., Wen, X.. Flexural wave propagation in beams with periodically attached vibration absorbers: band-gap behavior and band formation mechanisms. Journal of Sound and Vibration 2013;332(4):867–893.

[12] Zhu, R., Liu, X., Hu, G., Sun, C., Huang, G.. A chiral elastic metamaterial beam for broadband vibration suppression. Journal of Sound and Vibration 2014;333(10):2759–2773.

[13] Liu, Z., Zhang, X., Mao, Y., Zhu, Y., Yang, Z., Chan, C., et al. Locally resonant sonic materials. Science 2000;289(5485):1734–1736.

[14] Mace, B., Desmet, W., Pluymers, B.. Mid-frequency methods in sound and vibration—part a. Journal of Sound Vibration 2013;332:1895–1896.

[15] Denli, H., Sun, J.. Structural-acoustic optimization of sandwich structures with cellular cores for minimum sound radiation. Journal of Sound and Vibration 2007;301(1):93–105.

[16] Ouisse, M., Collet, M., Scarpa, F.. A piezo-shunted kirigami auxetic lattice for adaptive elastic wave filtering. Smart Materials and Structures 2016;25(11):115016.

[17] W. X. Zhong, F.W.W.. On the direct solution of wave propagation for repetitive structures. J Sound Vib 1995;181:485–501.

[18] Mencik, J.M., Ichchou, M.N.. Multi-mode propagation and diffusion in structures through finite elements. Eur J Mech A–Solid 2005;24(5):877–898.

[19] Mace, B.R., Duhamel, D., Brennan, M.J., Hinke, L.. Finite element prediction of wave motion in structural waveguides. J Acous Soc Am 2005;117:2835–2843.

[20] Trainiti, G., Rimoli, J., Ruzzene, M.. Wave propagation in periodically undulated beams and plates. International Journal of Solids and Structures 2015;75:260–276.

[21] Thierry, V., Brown, L., Chronopoulos, D.. Multi-scale wave propagation modelling for two-dimensional periodic textile composites. Composites Part B: Engineering 2018;150:144 – 156.

[22] Droz, C., Bareille, O., Ichchou, M.. A new procedure for the determination of structural characteristics of sandwich plates in medium frequencies. Composites Part B: Engineering 2017;112:103–111.

[23] Baid, H., Schaal, C., Samajder, H., Mal, A.. Dispersion of lamb waves in a honeycomb composite sandwich panel. Ultrasonics 2015;56:409–416.

[24] Serra, Q., Ichchou, M., Deü, J.F.. Wave properties in poroelastic media using a wave finite element method. Journal of Sound and Vibration 2015;335:125–146.

[25] Fabro, A.T., Ferguson, N.S., Jain, T., Halkyard, R., Mace, B.R.. Wave propagation in one-dimensional waveguides with slowly varying random spatially correlated variability. Journal of Sound and Vibration 2015;343:20–48.

[26] Souf, M.B., Bareille, O., Ichchou, M., Bouchoucha, F., Haddar, M.. Waves and energy in random elastic guided media through the stochastic wave finite element method. Physics Letters A 2013;377(37):2255–2264.

[27] Fan, Y., Collet, M., Ichchou, M., Li, L., Bareille, O., Dimitrijevic, Z.. A wave-based design of semi-active piezoelectric composites for broadband vibration control. Smart Materials and Structures 2016;25(5):055032.

[28] Nobrega, E., Gautier, F., Pelat, A., Dos Santos, J.. Vibration band gaps for elastic metamaterial rods using wave finite element method. Mechanical Systems and Signal Processing 2016;79:192–202.

[29] Claeys, C., de Melo Filho, N.G.R., Van Belle, L., Deckers, E., Desmet, W.. Design and validation of metamaterials for multiple structural stop bands in waveguides. Extreme Mechanics Letters 2017;12:7–22.

[30] Droz, C., Lainé, J.P., Ichchou, M., Inquiété, G.. A reduced formulation for the free-wave propagation analysis in composite structures. Compos Struct 2014;113:134–144.

[31] Zhou, C., Lainé, J., Ichchou, M., Zine, A.. Wave finite element method based on reduced model for one-dimensional periodic structures. International Journal of Applied Mechanics 2015;7(02):1550018.

[32] Droz, C., Zhou, C., Ichchou, M., Lainé, J.P.. A hybrid wave-mode formulation for the vibro-acoustic analysis of 2d periodic structures. Journal of Sound and Vibration 2016;363:285–302.

[33] Droz, C., Bareille, O., Lainé, J.P., Ichchou, M.. Wave-based shm of sandwich structures using cross-sectional waves. Structural Control and Health Monitoring 2018;25(2):e2085.

[34] Hasanian, M., Lissenden, C.J.. Second order harmonic guided wave mutual interactions in plate: Vector analysis, numerical simulation, and experimental results. Journal of Applied Physics 2017;122(8):084901.

[35] Liu, Y., Chillara, V.K., Lissenden, C.J.. On selection of primary modes for generation of strong internally resonant second harmonics in plate. Journal of Sound and Vibration 2013;332(18):4517–4528.

[36] Fromme, P., Wilcox, P.D., Lowe, M.J., Cawley, P.. On the development and testing of a guided ultrasonic wave array for structural integrity monitoring. ieee transactions on ultrasonics, ferroelectrics, and frequency control 2006;53(4):777–785.

[37] Zhou, W., Yuan, F.G., Shi, T.. Guided torsional wave generation of a linear in-plane shear piezoelectric array in metallic pipes. Ultrasonics 2016;65:69–77.

[38] Serey, V., Renier, M., Castaings, M., Masson, P., Quaegebeur, N., Micheau, P.. Selective Guided Waves Generation in a Bi-dimensional Waveguide for Damage Detection. Proceedings of the 11th International Workshop on Structural Health Monitoring 2017;1771–1778.

[39] Cooper, J., Hamilton, M., Wright, J.. Experimental evaluation of normal mode force appropriation methods using a rectangular plate. In: 10th International Modal Analysis Conference; vol. 1. 1992, p. 1327–1333.

[40] Wright, J., Cooper, J., Desforges, M.. Normal-mode force appropriation theory and application. Mechanical Systems and Signal Processing 1999;13(2):217–240.

[41] Ichchou, M., Bareille, O., Berthaut, J.. Identification of effective sandwich structural properties via an inverse wave approach. Engineering Structures 2008;30(10):2591–2604.

[42] Droz, C., Bareille, O., Ichchou, M.. Full wavefield measurement of transient wave pulses propagating in a composite panel. Data in Brief 2018;:(in Press).

[43] Piezoelectric solutions, pi ceramic gmbh. `http://www.pi-usa.us/pdf/PI_Piezoelectric_Solutions_Catalog.pdf`; 2016. Edition 12/2016.